

1 **Pumiliotoxin metabolism and molecular physiology in a poison frog**

2

3 Aurora Alvarez-Buylla¹, Cheyenne Y. Payne¹, Charles Vidoudez², Sunia A. Trauger² and Lauren

4 A. O'Connell*¹

5

6 1 Department of Biology, Stanford University, Stanford, CA 94305, USA

7 2 Harvard Center for Mass Spectrometry, Harvard University, Cambridge, MA 02138, USA

8

9 **Running title:** Physiology of pumiliotoxin uptake

10 **Word count (including methods): 2470**

11 **Word count (Abstract): 180**

12 **Key words:** alkaloid, cytochrome P450, allopumiliotoxin, RNA sequencing, Dendrobatidae,

13 decahydroquinoline

14

15 * To whom correspondence should be addressed:

16 Lauren A. O'Connell

17 Department of Biology

18 Stanford University

19 371 Jane Stanford Way

20 Stanford, CA 94305

21 loconnel@stanford.edu

22

23 **ABSTRACT**

24 Poison frogs bioaccumulate alkaloids for chemical defense from their arthropod diet. These
25 small molecules are sequestered from their gastrointestinal tract and transported to the skin for
26 storage. Although many alkaloids are accumulated without modification, some poison frog
27 species can metabolize pumiliotoxin (PTX **251D**) into the more potent allopumiliotoxin (aPTX
28 **267A**). Despite extensive research characterizing the chemical arsenal of poison frogs, the
29 physiological mechanisms involved in the sequestration and metabolism of individual alkaloids
30 is unknown. We performed a feeding experiment with the Dyeing poison frog (*Dendrobates*
31 *tinctorius*) to ask if this species can metabolize PTX **251D** into aPTX **267A** and what gene
32 expression changes are associated with PTX **251D** exposure in the intestines, liver, and skin.
33 We found that *D. tinctorius* can metabolize PTX **251D** into aPTX **267A**, and that PTX **251D**
34 exposure changed the expression of genes involved in immune system function and small
35 molecule metabolism and transport. These results show that individual alkaloids can modify
36 gene expression across poison frog tissues and suggest that different alkaloid classes in wild
37 diets may induce specific physiological changes for accumulation and metabolism.

38 1. INTRODUCTION

39 Poison frogs (Family Dendrobatidae) are chemically defended against predators [1–3]
40 using alkaloids that are sequestered from dietary arthropods [4,5]. Many poison frog alkaloids
41 have been found in the ants and mites they consume, suggesting most alkaloids are
42 sequestered unchanged [6–9]. However, poison frogs can also metabolize specific alkaloids into
43 more potent forms [10], although the underlying physiological mechanisms of this are unknown.
44 Controlled alkaloid-feeding experiments have been crucial in understanding alkaloid metabolism
45 in poison frogs [10–12]. Although many alkaloids are sequestered unmodified, some
46 dendrobatids metabolize pumiliotoxin (PTX) **251D** into the more potent allopumiliotoxin (aPTX)
47 **267A** [10]. After PTX **251D** feeding, both PTX **251D** and its metabolite, aPTX **267A**, were
48 detected on the skin of *Dendrobates auratus*, but only PTX **251D** was detected in *Phyllobates*
49 *bicolor* and *Epipedobates tricolor* [10]. These results suggest that an unidentified enzyme
50 performs the 7'-hydroxylation of PTX **251D** into aPTX **267A** in certain species. Whether other
51 poison frog species can metabolize PTX **251D** into aPTX **267A** remains unknown, along with
52 the metabolic mechanisms involved.

53 We conducted an alkaloid feeding study with the Dyeing poison frog (*Dendrobates*
54 *tinctorius*) to test whether this species can metabolize PTX **251D** into aPTX **267A** and to explore
55 gene expression changes associated with PTX **251D** exposure. To test whether PTX **251D**
56 elicited specific gene expression changes, we fed control frogs decahydroquinoline (DHQ) and
57 treatment frogs a mixture of PTX **251D** and DHQ. We predicted metabolic enzymes involved in
58 the hydroxylation of PTX **251D** into aPTX **267A** may be upregulated in response to their
59 metabolic target. Furthermore, if specific alkaloid sequestration pathways exist for PTX **251D**,
60 the proteins involved in that process may also be enriched upon exposure.

61 **2. MATERIALS AND METHODS**

62 **Alkaloid feeding**

63 Lab-reared (non-toxic) *Dendrobates tinctorius* were housed in terraria with live plants, a
64 water pool, and a shelter. Ten adult females were size-matched, randomly assigned to control
65 or experimental groups (N=5 per group), and then housed individually. To measure the specific
66 effects of PTX **251D** compared to a background toxicity, the control group was fed 0.01% DHQ
67 (Sigma-Aldrich, St. Louis, USA) in a solution of 1% EtOH and the experimental group was fed a
68 solution of 0.01% DHQ and 0.01% PTX (PepTech, Burlington, MA, USA) in a solution of 1%
69 EtOH. Each frog was fed 15 μ L each day for five days by pipetting the solution directly into the
70 mouth between 10am-12pm. On the afternoon of the fifth day, frogs were euthanized by cervical
71 transection and the dorsal skin, liver, intestines, and eggs were dissected into Trizol (Thermo
72 Fisher Scientific, Waltham, USA). All procedures were approved by the Institutional Animal Care
73 and Use Committee at Stanford University (protocol number #32870).

74 **RNA extraction and library preparation**

75 RNA extraction followed the protocol outlined in Caty *et al.* 2019 [13] and according to
76 the manufacturer's instructions. After the first spin, the organic layer was saved for alkaloid
77 extraction (see below). Poly-adenylated RNA was isolated using the NEXTflex PolyA Bead kit
78 (Bioo Scientific, Austin, USA) following manufacturer's instructions. RNA quality and lack of
79 ribosomal RNA was confirmed using an Agilent 2100 Bioanalyzer (Agilent Technologies, Santa
80 Clara, USA). Each RNA sequencing library was prepared using the NEXTflex Rapid RNAseq kit
81 (Bioo Scientific). Libraries were quantified with quantitative PCR (NEBnext Library quantification
82 kit, New England Biolabs, Ipswich, USA) and an Agilent Bioanalyzer High Sensitivity DNA chip,
83 both according to manufacturer's instructions. All libraries were pooled at equimolar amounts

84 and were sequenced on four lanes of an Illumina HiSeq 4000 machine to obtain 150 bp paired-
85 end reads.

86

87 **Transcriptome assembly and differential expression analysis**

88 All scripts are detailed in supplementary materials. We created a reference
89 transcriptome using Trinity [14], and cleaned the raw assembly by removing contigs with BLAST
90 hits belonging to microorganisms and invertebrates in the Swiss-Prot database [15].
91 Overlapping contigs were clustered using cd-hit-est [16,17] and contigs that were less than
92 250bp long were removed from the assembly. We mapped the paired quality-trimmed
93 sequences to the reference transcriptome using kallisto [18]. Samples were compared across
94 treatment groups (DHQ vs DHQ+PTX) for the skin, liver, and intestines, as these tissues
95 contained higher levels of PTX. Differences in gene expression levels were calculated using
96 DESeq2 [19] [$P < 0.05$ false discovery rate (Benjamini–Hochberg FDR), 4-fold change]. Contigs
97 with significant expression differences were BLAST-ed to the non-redundant (nr) database
98 using an E-value cutoff of $1e-5$. Many contigs did not have a BLAST hit, or aligned to
99 hypothetical or non-vertebrate proteins. Therefore, BLAST annotations were visually inspected
100 and contigs of interest were chosen based on candidates from existing literature. Boxplots were
101 made with R package ggplot2 (R version 3.6.3) using TMM (trimmed mean of M-values)
102 normalized expression.

103 **Alkaloid extraction and detection**

104 To isolate alkaloids, 0.3 mL of 100% EtOH was added to 1mL of organic layer from the
105 Trizol RNA extraction, inverted 10 times, and stored at room temperature for 2-3 minutes to
106 precipitate genomic DNA, which was pelleted by centrifugation at 2000g for 5 minutes at 4°C.
107 Then, 300 μ L of supernatant was transferred to a new microfuge tube. Proteins were
108 precipitated by adding 900 μ L of acetone, mixing by inversion for 10-15 seconds, incubating at

109 room temperature for 10 min, and centrifuging at max speed for 10 min at 4°C. Then, 1 mL of
110 supernatant was moved into a glass vial and stored at -20°C until dried down completely under
111 a gentle nitrogen gas flow.

112 Samples were resuspended in 200 µl of methanol:chloroform 1:1 and 1 µM Nicotine-d3
113 (used as an internal standard). A 10-point standard curve was prepared in the same solution
114 with DHQ and PTX. A QE+ mass spectrometer coupled to an Ultimate3000 LC (ThermoFisher)
115 was used for analysis. Five µl of each sample were injected on a single Gemini C18 column
116 (100x2mm, Phenomenex). The mobile phases were A: water and B: acetonitrile, both with 0.1%
117 formic acid. The gradient was 0% B for 1min, then increased to 100% B in 14 min, followed by 5
118 min at 100% B and 3.5 min at 0% B. Data were quantified using accurate mass, and specific
119 transitions for DHQ and PTX used the standard curve for absolute quantification. aPTX was
120 identified by accurate mass and MS/MS fragmentation similarity to PTX.

121 **Data analysis of liquid chromatography/tandem mass spectrometry (LC-MS/MS) data**

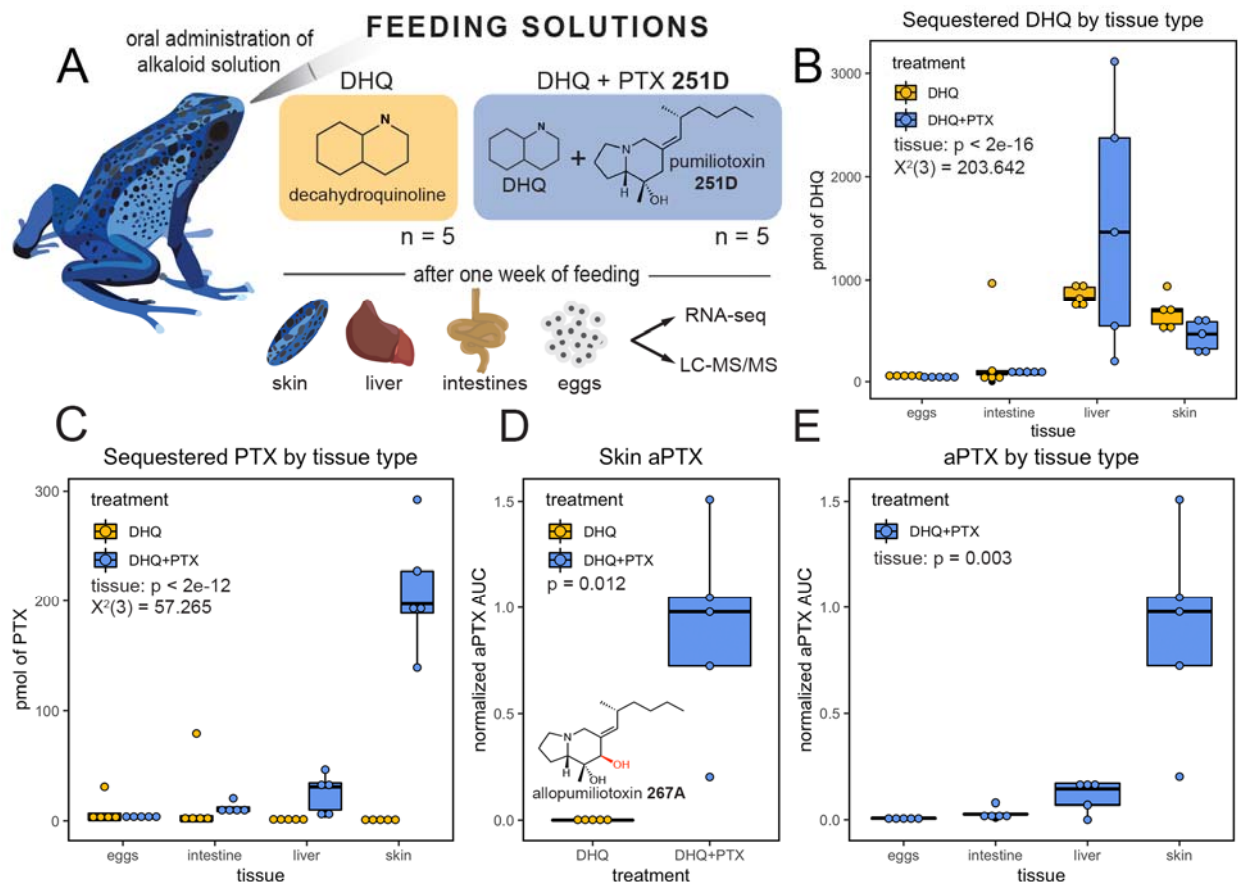
122 R version 3.6.3 was used for all statistical analyses. There were instances in the LC-
123 MS/MS data where the molecules of interest (DHQ, PTX **251D**, or aPTX **267A**) were not found,
124 and these were converted to zeros prior to statistical analyses. A generalized linear mixed
125 model was used (glmmTMB package in R) [20] to test for differences in alkaloid abundance
126 across tissues and treatment type, with the frog as a random effect and a negative binomial
127 error distribution. PTX **251D** and DHQ were analyzed separately. The aPTX **267A** abundance
128 was approximated using the area-under-the-curve divided by the internal nicotine standard, as
129 there is no standard for aPTX **267A**, and therefore exact pmol values could not be calculated. A
130 Wilcoxon rank-sum test (wilcox.test) was used to compare the aPTX values in the skin between
131 treatment groups and the Kruskal-Wallis test (kruskal.test) was used to compare the aPTX
132 values across tissues.

133

134 **3. RESULTS**

135 **The Dyeing poison frog metabolizes PTX to aPTX**

136 We conducted a feeding experiment to determine if the Dyeing poison frog can
137 metabolize PTX **251D** into aPTX **267A** (Figure 1A). Alkaloids were most abundant in the skin
138 and liver, followed by the intestines. Alkaloid abundance in the eggs was very low. DHQ
139 abundance did not differ by treatment group (GLMM treatment, $p = 0.377$), confirming that both
140 groups were fed equal amounts. DHQ abundance differed across tissue types (GLMM tissue, X^2
141 (3) = 203.642, $p < 2e-16$), with the highest levels occurring in the liver and skin (Figure 1B). PTX
142 **251D** abundance differed by tissue and treatment (GLMM tissue:treatment, X^2 (3) = 57.265, $p <$
143 $2e-12$), with the highest levels in the liver and skin in the DHQ+PTX feeding group (Figure 1C).
144 We detected aPTX **267A** in the skin of all individuals in the DHQ+PTX feeding group at higher
145 levels than the DHQ-fed group (Wilcoxon test, $W = 0$, $p = 0.012$, Figure 1D). The amount of
146 aPTX **267A** differed across tissues (Kruskal-Wallis, X^2 (3) = 13.727, $p = 0.003$), with the
147 abundance in the skin greater than eggs (post-hoc Dunn test, $p = 0.001$) and intestines (post-
148 hoc Dunn test, $p = 0.035$, Figure 1E). These data show *D. tinctorius* can metabolize PTX **251D**
149 into aPTX **267A** and that some alkaloid metabolism may occur in the liver and intestines.



150

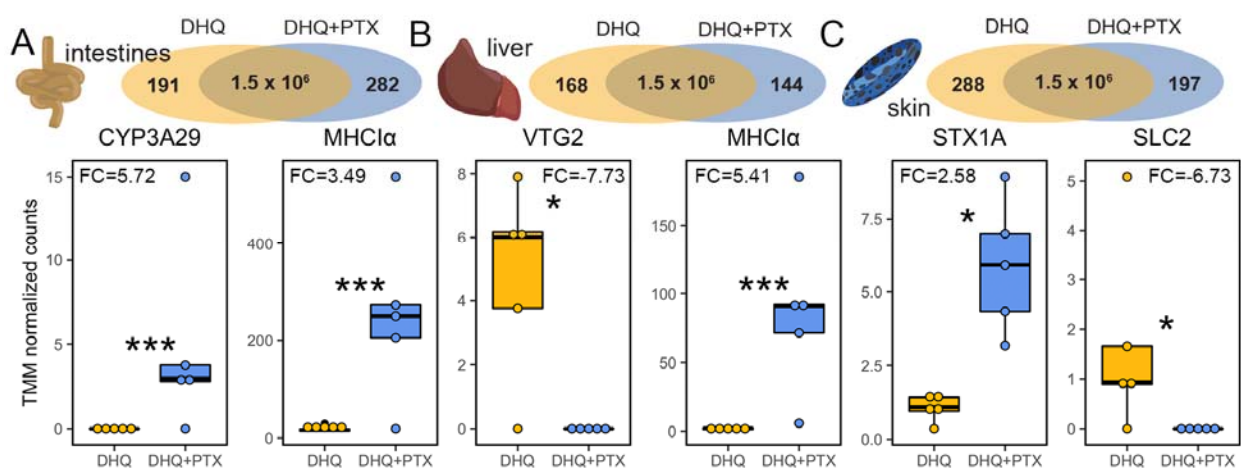
151 **Figure 1: Alkaloid sequestration in different tissue types.** (A) Frogs were orally
 152 administered either DHQ or DHQ+PTX once a day for five days. (B) DHQ abundance differed
 153 by tissue but not treatment group, and was highest in the liver and skin (GLMM tissue, $X^2(3) =$
 154 203.642 , $p < 2e-16$). (C) PTX levels differed by tissue and treatment, and were higher in the
 155 liver and skin of the DHQ+PTX fed group (GLMM tissue:treatment, $X^2(3) = 57.265$, $p < 2e-12$).
 156 (D) The hydroxylated metabolite aPTX was found in the DHQ+PTX fed frogs (Wilcoxon test, W
 157 $= 0$, p -value $= 0.012$, $n = 5$). (E) aPTX abundance differed across tissues within the DHQ-PTX
 158 group (Kruskal-Wallis, $X^2(3) = 13.727$, $p = 0.003$), and was found primarily in the skin, with
 159 some in the liver.

160

161 PTX alters gene expression across tissues

162 We next quantified gene expression changes associated with PTX sequestration and
 163 metabolism. Although hundreds of genes were differentially expressed in each tissue, most did
 164 not have annotations, or aligned with unknown, hypothetical, or non-vertebrate proteins.
 165 Cytochrome P450 (CYP3A29), an enzyme family well-known for their involvement in small
 166 molecule hydroxylation, was upregulated in the intestines ($\log_2FC = 5.72$, $p = 0.0045$; Figure

167 2A). In the liver, vitellogenin 2 (VTG2) was downregulated in the PTX feeding group ($\log_2FC = -$
 168 7.73, $p = 0.0421$, Figure 2B). MHC Class I α was upregulated in both the liver ($\log_2FC = 3.49$, p
 169 $= 0.0005$) and intestines ($\log_2FC = 5.41$, $p = 0.0001$) in the presence of PTX **251D** (Figure
 170 2A,B). In the skin, Syntaxin 1A (STX1A) was upregulated ($\log_2FC = 2.58$, $p = 0.0385$) and a
 171 Solute Carrier Family 2 protein (SLC2) was downregulated ($\log_2FC = 6.73$, $p = 0.0496$) in
 172 response to PTX **251D** (Figure 2C).



173
 174 **Figure 2: Differentially expressed genes in different tissues*.** (A) Differentially expressed
 175 genes in the intestines include CYP3A29, Cytochrome P450 Family 3 Protein 29 and MHC1 α ,
 176 MHC Class I alpha. (B) Differentially expressed genes in the liver included VTG2, vitellogenin 2
 177 and MHC1 α , MHC Class I alpha again. (C) Differentially expressed genes in the skin included
 178 STX1A, syntaxin 1A and SLC2, solute carrier family 2. (FC indicates \log_2 fold change values, *
 179 indicates adjusted p-value < 0.05, *** indicates adjusted p-value < 0.005) *Note: y-axis of
 180 individual plots have different scales
 181

182 4. DISCUSSION

183 Performing a controlled feeding study with DHQ and PTX **251D** allowed us to determine
 184 that *D. tinctorius* can metabolize PTX **251D** into aPTX **267A**. Although previous studies have
 185 documented wild *D. tinctorius* with aPTX on their skin [2,6], this is the first experimental
 186 evidence that this species metabolizes PTX **251D** into aPTX **267A**. The accumulation of both
 187 DHQ and PTX **251D** in the liver and intestines, along with the skin, indicates that these tissues
 188 play an important role in the sequestration of alkaloids. Indeed, the liver and intestines are

189 important sites of alkaloid metabolism in mammals due to high levels of Cytochrome P450s [21–
190 23]. Together, these results show that *D. tinctorius* is able to metabolize PTX **251D** into aPTX
191 **267A** and that the tissue distribution of alkaloids includes the skin, liver, and intestines. In the
192 future, a better understanding of alkaloid pharmacokinetics could be achieved through finer
193 time-course feeding experiments.

194 PTX **251D** feeding changed gene expression in the intestines, liver, and skin, suggesting
195 a single alkaloid can change poison frog physiology. Specifically, the upregulation of CYP3A29
196 in response to PTX in the intestines implicates this enzyme in the metabolism of PTX **251D** into
197 aPTX **267A**, or of PTX into a metabolic byproduct to be later discarded. Although we originally
198 expected to identify metabolism enzymes in the liver, it is possible the liver instead acts as a
199 detoxification site. In the dendrobatid *Oophaga sylvatica*, feeding DHQ compared to a non-
200 alkaloid vehicle control led to a downregulation of CYP3A29 in the intestines, suggesting that
201 expression is regulated differently by specific alkaloids [24]. The upregulation of MHC class I α
202 proteins in the intestines and liver in response to PTX **251D** supports previous findings that frog
203 immune systems respond to alkaloids [13,25]. We also found VTG2 (vitellogenin-2) was
204 downregulated in response to PTX **251D**. Although vitellogenins are typically thought to be egg-
205 yolk proteins, they also play regulatory roles and protect cells from reactive oxygen species that
206 may arise from alkaloid metabolism [26–28]. Finally, SLC2 (solute carrier family 2) which
207 encodes for the GLUT family of glucose transporters, was downregulated in the skin with PTX
208 feeding. Alkaloids have been found to be potent inhibitors of GLUTs in mammalian cell lines,
209 and the downregulation of GLUTs in this case may be due to the presence of concentrated PTX
210 **251D** in the frog skin [29]. Together, these data support an argument for physiological “fine-
211 tuning” of gene expression in response to certain alkaloids.

212 We provide evidence that *D. tinctorius* can metabolize PTX **251D** into aPTX **267A** and
213 that PTX **251D** exposure changes gene expression across tissues, demonstrating that specific
214 alkaloids can change poison frog physiology [24,25]. Following up on candidate genes with

215 biochemical studies is needed in order to fully characterize the genetics of alkaloid
216 sequestration and metabolism. In the wild, where chemically defended dendrobatids carry many
217 different alkaloids, subtle alkaloid differences may induce distinct gene expression changes.
218 More broadly, modulating gene expression in response to specific alkaloids may set the stage
219 for local adaptation to environmental resources.

220 **5. ACKNOWLEDGEMENTS**

221 We thank Stephanie Caty and Nora Moskowitz for their comments. We acknowledge that the
222 land on which this research was conducted is the ancestral and unceded land of the Muwekma
223 Ohlone tribe.

224

225 **6. FUNDING**

226 This work was supported by a National Science Foundation (NSF) [IOS-1822025] grant
227 to LAO. AAB is supported by a NSF Graduate Research Fellowship (DGE-1656518) and an
228 HHMI Gilliam Fellowship. LAO is a New York Stem Cell – Robertson Investigator.

229

230 **6. DATA ACCESSIBILITY**

231 All LC-MS/MS data from the alkaloid analysis is available from the Dryad Digital Repository
232 (pending). All Illumina fastq files are available on the Sequence Read Archive (pending). All
233 data and code is available in the supplementary material.

234 **7. AUTHOR CONTRIBUTIONS**

235 AAB and LAO designed the experiment. AAB and CYP carried out the experimental procedures.
236 CV and SAT quantified alkaloids. AAB analyzed the data. AAB and LAO wrote the manuscript
237 with contributions from all authors.

238 8. REFERENCES

- 239 1. Daly JW, Brown GB, Mensah-Dwumah M, Myers CW. 1978 Classification of skin alkaloids
240 from neotropical poison-dart frogs (dendrobatidae). *Toxicon* **16**, 163–188.
- 241 2. Daly JW, Myers CW, Whittaker N. 1987 Further classification of skin alkaloids from
242 neotropical poison frogs (dendrobatidae), with a general survey of toxic/noxious substances
243 in the amphibia. *Toxicon* **25**, 1023–1095.
- 244 3. Daly JW, Spande TF, Garraffo HM. 2005 Alkaloids from Amphibian Skin: A Tabulation of
245 Over Eight-Hundred Compounds. *J. Nat. Prod.* **68**, 1556–1575.
- 246 4. Darst CR, Menéndez-Guerrero PA, Coloma LA, Cannatella DC. 2004 Evolution of dietary
247 specialization and chemical defense in poison frogs (Dendrobatidae): a comparative
248 analysis. *Am. Nat.* **165**, 56–69.
- 249 5. Daly JW, Garraffo HM, Spande TF, Jaramillo C, Rand AS. 1994 Dietary source for skin
250 alkaloids of poison frogs (Dendrobatidae)? *J. Chem. Ecol.* **20**, 943–955.
- 251 6. Saporito RA, Garraffo HM, Donnelly MA, Edwards AL, Longino JT, Daly JW. 2004
252 Formicine ants: An arthropod source for the pumiliotoxin alkaloids of dendrobatid poison
253 frogs. *Proc. Natl. Acad. Sci. U. S. A.* **101**, 8045–8050.
- 254 7. Saporito RA, Donnelly MA, Norton RA, Garraffo HM, Spande TF, Daly JW. 2007 Oribatid
255 mites as a major dietary source for alkaloids in poison frogs. *Proceedings of the National
256 Academy of Sciences* **104**, 8885–8890.
- 257 8. Moskowitz NA *et al.* 2020 Land use impacts poison frog chemical defenses through
258 changes in leaf litter ant communities. *Neotropical Biodiversity* **6**, lxxv–lxxxvii.
- 259 9. McGugan JR, Byrd GD, Roland AB, Caty SN, Kabir N, Tapia EE, Trauger SA, Coloma LA,
260 O’Connell LA. 2016 Ant and Mite Diversity Drives Toxin Variation in the Little Devil Poison
261 Frog. *J. Chem. Ecol.* **42**, 537–551.
- 262 10. Daly JW, Garraffo HM, Spande TF, Clark VC, Ma J, Ziffer H, Cover JF. 2003 Evidence for
263 an enantioselective pumiliotoxin 7-hydroxylase in dendrobatid poison frogs of the genus
264 *Dendrobates*. *Proceedings of the National Academy of Sciences* **100**, 11092–11097.
- 265 11. Daly JW, Secunda SI, Garraffo HM, Spande TF, Wisnieski A, Cover JF. 1994 An uptake
266 system for dietary alkaloids in poison frogs (Dendrobatidae). *Toxicon* **32**, 657–663.
- 267 12. Saporito RA, Spande TF, Martin Garraffo H, Donnelly MA. 2009 Arthropod Alkaloids in
268 Poison Frogs: A Review of the ‘Dietary Hypothesis’. *HETEROCYCLES*. **79**, 277.
269 (doi:10.3987/rev-08-sr(d)11)
- 270 13. Caty SN *et al.* 2019 Molecular physiology of chemical defenses in a poison frog. *J. Exp.*
271 *Biol.* **222**, jeb204149.
- 272 14. Haas BJ *et al.* 2013 De novo transcript sequence reconstruction from RNA-seq using the
273 Trinity platform for reference generation and analysis. *Nat. Protoc.* **8**, 1494–1512.
- 274 15. UniProt Consortium. 2019 UniProt: a worldwide hub of protein knowledge. *Nucleic Acids*

- 275 *Res.* **47**, D506–D515.
- 276 16. Li W, Godzik A. 2006 Cd-hit: a fast program for clustering and comparing large sets of
277 protein or nucleotide sequences. *Bioinformatics*. **22**, 1658–1659.
278 (doi:10.1093/bioinformatics/btl158)
- 279 17. Fu L, Niu B, Zhu Z, Wu S, Li W. 2012 CD-HIT: accelerated for clustering the next-
280 generation sequencing data. *Bioinformatics* **28**, 3150–3152.
- 281 18. Bray NL, Pimentel H, Melsted P, Pachter L. 2016 Erratum: Near-optimal probabilistic RNA-
282 seq quantification. *Nat. Biotechnol.* **34**, 888.
- 283 19. Love MI, Huber W, Anders S. 2014 Moderated estimation of fold change and dispersion for
284 RNA-seq data with DESeq2. *Genome Biol.* **15**, 550.
- 285 20. Brooks M *et al.* 2017 glmmTMB Balances Speed and Flexibility Among Packages for Zero-
286 inflated Generalized Linear Mixed Modeling. *The R Journal*. **9**, 378. (doi:10.32614/rj-2017-
287 066)
- 288 21. Grant DM. 1991 Detoxification pathways in the liver. *J. Inherit. Metab. Dis.* **14**, 421–430.
- 289 22. Robinson T. 2000 The Metabolism and Biochemical Actions of Alkaloids in Animals.
290 *Bioactive Natural Products (Part C)*. , 3–54. (doi:10.1016/s1572-5995(00)80022-8)
- 291 23. Thelen K, Dressman JB. 2009 Cytochrome P450-mediated metabolism in the human gut
292 wall. *J. Pharm. Pharmacol.* **61**, 541–558.
- 293 24. O’Connell LA, Course, LS50: Integrated Science Laboratory, O’Connell JD, Paulo JA,
294 Trauger SA, Gygi SP, Murray AW. 2020 Rapid toxin sequestration impacts poison frog
295 physiology. *bioRxiv* , 2020.05.27.119081.
- 296 25. Sanchez E *et al.* 2019 Transcriptomic Signatures of Experimental Alkaloid Consumption in
297 a Poison Frog. *Genes* **10**, 733.
- 298 26. Havukainen H, Münch D, Baumann A, Zhong S, Halskau Ø, Krogsgaard M, Amdam GV.
299 2013 Vitellogenin recognizes cell damage through membrane binding and shields living
300 cells from reactive oxygen species. *J. Biol. Chem.* **288**, 28369–28381.
- 301 27. Nunes FMF, Ihle KE, Mutti NS, Simões ZLP, Amdam GV. 2013 The gene vitellogenin
302 affects microRNA regulation in honey bee (*Apis mellifera*) fat body and brain. *J. Exp. Biol.*
303 **216**, 3724–3732.
- 304 28. Seehuus S-C, Norberg K, Gimsa U, Krekling T, Amdam GV. 2006 Reproductive protein
305 protects functionally sterile honey bee workers from oxidative stress. *Proc. Natl. Acad. Sci.*
306 *U. S. A.* **103**, 962–967.
- 307 29. Reckzeh ES, Waldmann H. 2020 Development of Glucose Transporter (GLUT) Inhibitors.
308 *European J. Org. Chem.* **2020**, 2321–2329.
- 309